Computer Simulations of 3d Lorentzian Quantum Gravity

J. Ambjørn[a][*][‡], J. Jurkiewicz[b][*][†][‡] and R. Loll[c][‡]

[a]The Niels Bohr Institute, Blegdamsvej 17, DK-2100 Copenhagen Ø, Denmark

[b]Institute of Physics, Jagellonian University, Reymonta 4, PL 30-059 Krakow, Poland

[c]Albert-Einstein-Institut, Max-Planck-Institut für Gravitationsphysik,
Am Mühlenberg 1, D-14476 Golm, Germany

We investigate the phase diagram of non-perturbative three-dimensional Lorentzian quantum gravity with the help of Monte Carlo simulations. The system has a first-order phase transition at a critical value k_0^c of the bare inverse gravitational coupling constant k_0. For $k_0 > k_0^c$ the system reduces to a product of uncorrelated Euclidean 2d gravity models and has no intrinsic interest as a model of 3d gravity. For $k_0 < k_0^c$, extended three-dimensional geometries dominate the functional integral despite the fact that we perform a sum over geometries and no particular background is distinguished at the outset. Furthermore, all systems with $k_0 < k_0^c$ have the same continuum limit. A different choice of k_0 corresponds merely to a redefinition of the overall length scale.

1. INTRODUCTION

We still need to find *the theory of quantum gravity*. In [1,2] we have proposed a dynamically triangulated model of two, three and four dimensional quantum gravity with the following properties:
(a) Lorentzian space-time geometries (histories) are obtained by causally gluing sets of Lorentzian building blocks, i.e. d-dimensional simplices with simple length assignments;
(b) all histories have a preferred discrete notion of proper time t; t counts the number of evolution steps of a transfer matrix between adjacent spatial slices, the latter given by $(d-1)$-dimensional triangulations of equilateral Euclidean simplices;
(c) each Lorentzian discrete geometry can be "Wick-rotated" to a Euclidean one, defined on the same (topological) triangulation;
(d) at the level of the discretized action, the "Wick rotation" is achieved by an analytic continuation in the dimensionless ratio $\alpha = -l_t^2/l_s^2$ of the squared time- and space-like link length; for $\alpha = -1$ one obtains the usual Euclidean action of dynamically triangulated gravity;
(e) the extreme phases of degenerate geometries found in the Euclidean models cannot be realized in the Lorentzian case.

A metric space-time is constructed by "filling in" for all t the d-dimensional sandwich between the pair of spatial slices at integer times t and $t+1$. We only consider regular gluings which lead to *simplicial manifolds*. In the case of *three*-dimensional quantum gravity the basic building blocks are three types of Lorentzian tetrahedra, (1): (3,1)-tetrahedra (three vertices contained in slice t and one vertex in slice $t+1$): they have three space- and three time-like edges; their number in the sandwich $[t, t+1]$ will be denoted by $N_{31}(t)$; (2): (1,3)-tetrahedra: the same as above, but upside-down; the tip of the tetrahedron is at t and its base lies in the slice $t+1$; notation $N_{13}(t)$; (3): (2,2)-tetrahedra: one edge (and therefore two vertices) at each t and $t+1$; they have two space- and four time-like edges; notation $N_{22}(t)$.

Each of these triangulated space-times carries a causal structure defined by the piecewise flat Lorentzian metric. Each time-like link is given a future-orientation in the positive t-direction, so

that two lattice vertices connected by a sequence of positively oriented links are causally related.

As mentioned in (d) above, after rotating to Euclidean signature and choosing $\alpha = -1$, the Einstein action becomes identical to the action

$$S_{\mathrm{E}}(N_0, N_3, T) = -k_0 N_0 + k_3 N_3 \qquad (1)$$

used in Euclidean dynamical triangulations [3], where N_0 and N_3 denote the total numbers of vertices and tetrahedra in the triangulation. The dimensionless couplings k_0 and k_3 have been introduced to conform with the conventions used in 3d *Euclidean* simplicial quantum gravity. Here k_0 is proportional to the bare inverse gravitational coupling constant, while k_3 is a linear combination of the bare cosmological and inverse gravitational constants. In a slight abuse of language, we will still refer to k_3 as the (bare) cosmological constant. We fix the space-time topology to $S^1 \times S^2$, where the periodic identification in the t-direction has been chosen entirely for practical convenience. The total length of the space-time in the compactified S^1-direction (i.e. the number of proper-time steps) is denoted by T. The partition function is thus

$$Z(k_0, k_3, T) = \sum_{\mathcal{T}_T(S^1 \times S^2)} \mathrm{e}^{-S_{\mathrm{E}}(N_0, N_3, T)}, \qquad (2)$$

where the sum is taken over the class $\mathcal{T}_T(S^1 \times S^2)$ of triangulations of $S^1 \times S^2$ specified earlier, for fixed T. While (2) is similar in structure to the standard partition function of dynamically triangulated Euclidean gravity, one should bear in mind that the set of triangulations contributing in (2) is quite different.

2. THE MONTE CARLO SIMULATION

We explore the phase diagram of the theory defined by the state sum (2) using Monte Carlo simulations. A 3d triangulation in the sum (2) consists of t successive 2d triangulations. These spatial slices are glued together by filling the space-time gaps between them with the three types of building blocks described in the introduction.

A local updating algorithm consisting of five basic *moves* changes one such triangulation into another one, while preserving the constant-time

slice structure. A successive application of these moves will take us around in the class of triangulation with fixed T. The moves are (see [4] for more details):

(1): consider two neighbouring triangles in the spatial t-plane such that the two associated pairs of tetrahedra above and below the t-plane each share one triangle. We can perform a standard "flip" move of the link common to the two triangles in the t-plane and make a corresponding reassignment of tetrahedra. (2&3): Consider a triangle in the spatial t-plane and insert a vertex at its centre. In this way the two neighbouring tetrahedra sharing the triangle are replaced by six tetrahedra, three above and three below. There is an obvious inverse move. (4&5): The fourth move is the standard Alexander move performed on a (2,2)-tetrahedron and a (3,1)-tetrahedron sharing a triangle, replacing it by two (2,2)- and one (3,1)-tetrahedra, and the fifth move is its inverse. Obviously the (3,1)-tetrahedron could have been replaced by a (1,3)-tetrahedron in (4&5).

The strategy for the simulations is the usual one from dynamical triangulations: fine-tune the cosmological constant to its critical value $k_3^c(k_0)$ (which depends on the bare inverse gravitational coupling constant k_0) and keep the fluctuations of space-time volume bounded within a certain range. Then measure expectation values of suitable observables for these quantum universes.

3. RESULTS

In order to explore the phase diagram of our regularized model we have to identify an order parameter, and explore how it changes with the coupling constant, in this case k_0. We have found that the ratio τ between the total number N_{22} of (2,2)-tetrahedra and the total space-time volume

$$N_3 \equiv N_{tot} = N_{22} + N_{31} + N_{13}$$

serves as an efficient order parameter. In Fig. 1 we show τ as a function of k_0. One observes a rapid drop to zero of $\tau(k_0)$ around $k_0 \approx 6.64$. Increasing N_3, the drop becomes a jump, typical for a first-order phase transition. A detailed study of the neighbourhood of $k_0 = 6.64$ reveals a hysteresis as one performs a cycle, moving above

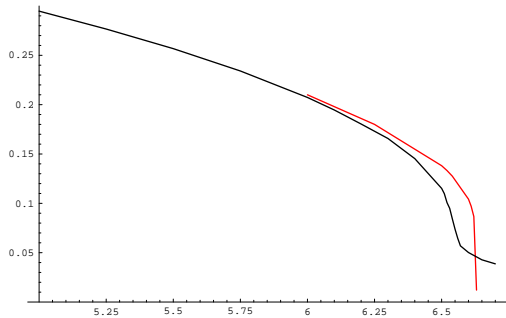and below the critical value k_0^c, again as expected from a first-order transition.

Figure 1. The order parameter $\tau = N_{22}/N_{tot}$ for configurations with $T = 64$, and $N_3 = 16,000$ (black curve) and 64,000 (red curve), plotted as a function of k_0.

The phase above k_0^c is of no interest for continuum 3d quantum gravity since one can show that it is equivalent to an uncorrelated product of 2d Euclidean gravity models [4].

We now turn to the interesting phase of $k_0 < k_0^c$. Remarkably, we observe here the emergence of well-defined three-dimensional configurations. In Fig. 2 we present a snapshot of a configuration of 16,000 tetrahedra for $k_0 = 5.0$ and of total proper-time extent $T = 32$. It shows the 2d spatial volume as a function of the time t. Following the computer-time history of this extended object, it is clear that although it does indeed fluctuate, the fluctuations take place around a three-dimensional object of a well-defined linear extension. *The emergence of a ground state of extended geometry is a very non-trivial property of the model, since we never put in any preferred background geometry by hand.* No structures of this kind have ever been observed in dynamically triangulated models of *Euclidean* quantum gravity. It underscores the fact that the Lorentzian models are genuinely different and affirms our conjecture that in $d \geq 3$ they are less pathological than their Euclidean counterparts. Let us denote the typical time-extent of our extended "universe" by T_u. We will always choose the total
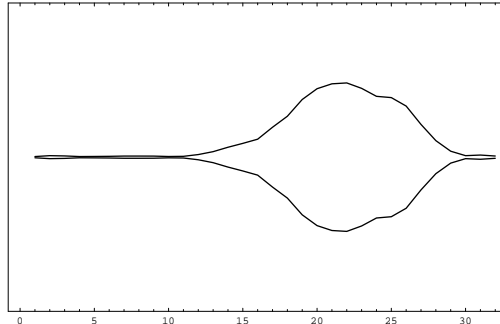

Figure 2. Snapshot of the distribution of 2d volumes $N_{31}(t)$ of spatial slices at times $t \in [0, T]$, with $T = 32$ and $k_0 = 5.0$ ($k_0^c = 6.64$).

proper time T sufficiently large, such that $T_u < T$ for the range of N_3 under consideration. Since both the shape of the universe and its location along the t-direction fluctuate, we have found it convenient to measure the correlation function

$$C(\Delta) = \frac{1}{T^2} \sum_{t=1}^{T} \langle N_{2s}(t) N_{2s}(t + \Delta) \rangle, \qquad (3)$$

where $N_{2s}(t) = N_{13}(t) + N_{31}(t) + N_{22}(t)$, as a function of the displacement Δ to determine the scaling of T_u with the space-time volume N_3. This correlator has the advantage of being translation-invariant in t and allows for a precise measurement by averaging over many independent configurations. From the typical shape of the space-time configurations we expect $C(\Delta)$ to be of the order of the spatial cut-off if $\Delta \gg 2T_b$. Fig. 3 illustrates the result of our measurements of $C(\Delta)$, with the dots representing the measured values. The theoretical curve to which we are fitting corresponds to a sphere S^3 with the radius as a free parameter. (By S^3 we mean the 3d geometry of constant positive curvature which is a *classical* solution of Euclidean gravity with a positive cosmological constant.) In order to "adapt" the S^3-solution to the topology $S^1 \times S^2$, we assume that the standard S^3-solution is valid until the radius r of the S^2-slice reaches the spatial cut-off scale. Beyond this point, the value of r is frozen to the cut-off value, which we also take
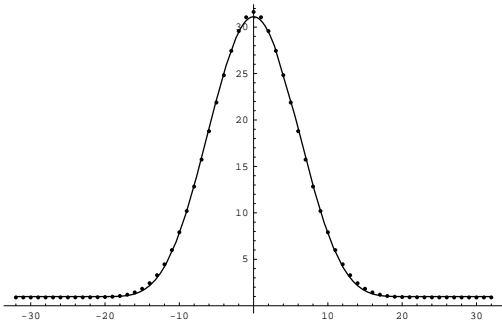
Figure 3. The correlator $C(\Delta)$ with $T = 64$ and $N_3 = 32,000$. Dots are the measured values (error bars less than dots), and the curve is fitted from the sphere solution described in the text.

as a free parameter. For this "spherical" geometry we then perform the integral (the sum) in (3), without the average $\langle \cdot \rangle$. As is evident from Fig. 3, the volume distribution associated with this fixed geometry gives a rather good fit to our data. This provides some evidence that we can ignore the quantum average implied by $\langle \cdot \rangle$, and that our universes behave semi-classically, *at least as far as their macroscopic geometric properties are concerned*. We should mention that our "S^3-solution" is not singled out uniquely, since the choice of a Gaussian shape in the t-direction gives a fit of comparable quality.

For various space-time volumes N_3 (typically 8, 16, 32 and 64k) we have determined the radius R_{S^3} of S^3 from the fits to the measured $C(\Delta)$. From this, we have finally found $\alpha = 0.34 \pm 0.02$ as the best exponent in the scaling relation

$$R_{S^3}(N_3) = N_3^\alpha. \tag{4}$$

The same value is obtained using other ways to extract T_u, lending additional support to the genuinely three-dimensional nature of our universes.

Another important result concerns the relation between the geometries of different k_0, in the phase where $k_0 < k_0^c$. In the numerical simulations we have observed the following: (i) the distributions as functions of t can be made to coincide for different k_0 by rescaling the time,

$t \to f_{ti}(k_0)t$ or $a_t \to f_{ti}(k_0)a_t$, where a_t is the link length in time direction. (ii) The distributions measured in the spatial slices from *inside* the universe can be made to coincide for different k_0 by rescaling the spatial link distance $a_s \to f_{sp}(k_0)a_s$, where a_s is the length of the spatial links. This is illustrated in Fig. 4 for the distributions of 2d volumes $V(l)$ of *spatial* spherical shells of (link) radius l, measured for various values of k_0. (iii) Within the numerical accuracy
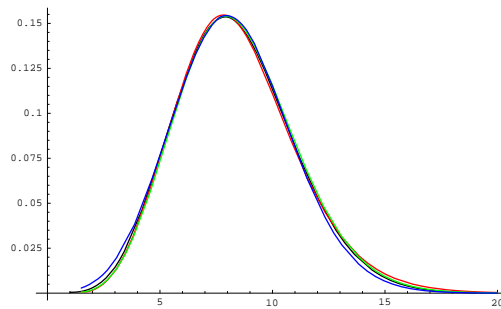

Figure 4. The 2d volume $V(l)$ of spatial spherical shells, measured only on slices inside the spherical universe, for various k_0 and rescaled, using the seemingly unrelated scaling obtained by applying the same philosophy to the correlator $C(\Delta)$.

we find that $f_{ti}(k_0) = f_{sp}(k_0)$.

We conclude that apart from the overall length scale of the universe, set by the bare inverse gravitational coupling k_0, *the physics is the same for all values k_0 below k_0^c*.

REFERENCES

1. J. Ambjørn and R. Loll, Nucl. Phys. B536 (1998) 407.
2. J. Ambjørn, J. Jurkiewicz and R. Loll, Phys. Rev. Lett. 85 (2000) 924.
3. J. Ambjørn and J. Jurkiewicz, Phys. Lett. B278 (1992) 42.
4. J. Ambjørn, J. Jurkiewicz and R. Loll, *Nonperturbative 3d Lorentzian quantum gravity*, to appear.

Elsevier instructions for the preparation of a 2-column format camera-ready paper in LaTeX

P. de Groot[a*], R. de Maas[a†], X.-Y. Wang[b] and A. Sheffield[a‡]

[a]Mathematics and Computer Science Division, Elsevier Science Publishers B.V.,
P.O. Box 103, 1000 AC Amsterdam, The Netherlands

[b]Economics Department, University of Winchester,
2 Finch Road, Winchester, Hampshire P3L T19, United Kingdom

These pages provide you with an example of the layout and style for 100% reproduction which we wish you to adopt during the preparation of your paper. This is the output from the LaTeX document class you requested.

1. FORMAT

Text should be produced within the dimensions shown on these pages: each column 7.5 cm wide with 1 cm middle margin, total width of 16 cm and a maximum length of 20.2 cm on first pages and 21 cm on second and following pages. The LaTeX document class uses the maximal stipulated length apart from the following two exceptions (i) LaTeX does not begin a new section directly at the bottom of a page, but transfers the heading to the top of the next page; (ii) LaTeX never (well, hardly ever) exceeds the length of the text area in order to complete a section of text or a paragraph. Here are some references: [1,2].

1.1. Spacing

We normally recommend the use of 1.0 (single) line spacing. However, when typing complicated mathematical text LaTeX automatically increases the space between text lines in order to prevent sub- and superscript fonts overlapping

---

*Footnotes should appear on the first page only to indicate your present address (if different from your normal address), research grant, sponsoring agency, etc. These are obtained with the \thanks command.

†For following authors with the same address use the \addressmark command.

‡To reuse an addressmark later on, label the address with an optional argument to the \address command, e.g. \address[MCSD], and repeat the label as the optional argument to the \addressmark command, e.g. \addressmark[MCSD].

---

one another and making your printed matter illegible.

1.2. Fonts

These instructions have been produced using a 10 point Computer Modern Roman. Other recommended fonts are 10 point Times Roman, New Century Schoolbook, Bookman Light and Palatino.

2. PRINTOUT

The most suitable printer is a laser printer. A dot matrix printer should only be used if it possesses an 18 or 24 pin printhead ("letter-quality").

The printout submitted should be an original; a photocopy is not acceptable. Please make use of good quality plain white A4 (or US Letter) paper size. *The dimensions shown here should be strictly adhered to: do not make changes to these dimensions, which are determined by the document class.* The document class leaves at least 3 cm at the top of the page before the head, which contains the page number.

Printers sometimes produce text which contains light and dark streaks, or has considerable lighting variation either between left-hand and right-hand margins or between text heads and bottoms. To achieve optimal reproduction quality, the contrast of text lettering must be uniform, sharp and dark over the whole page and through-

out the article.

If corrections are made to the text, print completely new replacement pages. The contrast on these pages should be consistent with the rest of the paper as should text dimensions and font sizes.

3. TABLES AND ILLUSTRATIONS

Tables should be made with LaTeX; illustrations should be originals or sharp prints. They should be arranged throughout the text and preferably be included *on the same page as they are first discussed*. They should have a self-contained caption and be positioned in flush-left alignment with the text margin within the column. If they do not fit into one column they may be placed across both columns (using \begin{table*} or \begin{figure*} so that they appear at the top of a page).

3.1. Tables

Tables should be presented in the form shown in Table 1. Their layout should be consistent throughout.

Horizontal lines should be placed above and below table headings, above the subheadings and at the end of the table above any notes. Vertical lines should be avoided.

If a table is too long to fit onto one page, the table number and headings should be repeated above the continuation of the table. For this you have to reset the table counter with \addtocounter{table}{-1}. Alternatively, the table can be turned by 90° ('landscape mode') and spread over two consecutive pages (first an even-numbered, then an odd-numbered one) created by means of \begin{table}[h] without a caption. To do this, you prepare the table as a separate LaTeX document and attach the tables to the empty pages with a few spots of suitable glue.

3.2. Useful table packages

Modern LaTeX comes with several packages for tables that provide additional functionality. Below we mention a few. See the documentation of the individual packages for more details. The packages can be found in LaTeX's tools directory.

Table 2: The next-to-leading order (NLO) results *without* the pion field.

Λ (MeV)	140	150	175	200	225	250	Exp.	v_{18} [?]
r_d (fm)	1.973	1.972	1.974	1.978	1.983	1.987	1.966(7)	1.967
Q_d (fm^2)	0.259	0.268	0.287	0.302	0.312	0.319	0.286	0.270
P_D (%)	2.32	2.83	4.34	6.14	8.09	9.90	–	5.76
μ_d	0.867	0.864	0.855	0.845	0.834	0.823	0.8574	0.847
$\mathcal{M}_{\mathrm{M1}}$ (fm)	3.995	3.989	3.973	3.955	3.936	3.918	–	3.979
$\mathcal{M}_{\mathrm{GT}}$ (fm)	4.887	4.881	4.864	4.846	4.827	4.810	–	4.859
$\delta_{\mathrm{1B}}^{\mathrm{VP}}$ (%)	−0.45	−0.45	−0.45	−0.45	−0.45	−0.44	–	−0.45
$\delta_{\mathrm{1B}}^{\mathrm{C2:C}}$ (%)	0.03	0.03	0.03	0.03	0.03	0.03	–	0.03
$\delta_{\mathrm{1B}}^{\mathrm{C2:N}}$ (%)	−0.19	−0.19	−0.18	−0.15	−0.12	−0.10	–	−0.21

The experimental values are given in ref. [4].

Table 1
The next-to-leading order (NLO) results *without* the pion field.

Λ (MeV)	140	150	175	200
r_d (fm)	1.973	1.972	1.974	1.978
Q_d (fm^2)	0.259	0.268	0.287	0.302
P_D (%)	2.32	2.83	4.34	6.14
μ_d	0.867	0.864	0.855	0.845
$\mathcal{M}_{\mathrm{M1}}$ (fm)	3.995	3.989	3.973	3.955
$\mathcal{M}_{\mathrm{GT}}$ (fm)	4.887	4.881	4.864	4.846
$\delta_{1B}^{\mathrm{VP}}$ (%)	-0.45	-0.45	-0.45	-0.45
$\delta_{1B}^{\mathrm{C2:C}}$ (%)	0.03	0.03	0.03	0.03
$\delta_{1B}^{\mathrm{C2:N}}$ (%)	-0.19	-0.19	-0.18	-0.15

The experimental values are given in ref. [4].

array Various extensions to LaTeX's `array` and `tabular` environments.

longtable Automatically break tables over several pages. Put the table in the `longtable` environment instead of the `table` environment.

dcolumn Define your own type of column. Among others, this is one way to obtain alignment on the decimal point.

tabularx Smart column width calculation within a specified table width.

rotating Print a page with a wide table or figure in landscape orientation using the `sidewaystable` or `sidewaysfigure` environments, and many other rotating tricks. Use the package with the `figuresright` option to make all tables and figures rotate in clockwise. Use the starred form of the `sideways` environments to obtain full-width tables or figures in a two-column article.

3.3. Line drawings

Line drawings should be drawn in India ink on tracing paper with the aid of a stencil or should be glossy prints of the same; computer prepared drawings are also acceptable. They should be attached to your manuscript page, correctly aligned, using suitable glue and *not transparent tape.* When placing a figure at the top of a page, the top of the figure should be at the same level as the bottom of the first text line.

All notations and lettering should be no less than 2 mm high. The use of heavy black, bold lettering should be avoided as this will look unpleasantly dark when printed.

3.4. PostScript figures

Instead of providing separate drawings or prints of the figures you may also use PostScript files which are included into your LaTeX file and printed together with the text. Use one of the packages from LaTeX's `graphics` directory: `graphics`, `graphicx` or `epsfig`, with the `\usepackage` command, and then use the appropriate commands (`\includegraphics` or `\epsfig`) to include your PostScript file.

The simplest command is:
`\includegraphics{file}`, which inserts the PostScript file `file` at its own size. The starred version of this command:
`\includegraphics*{file}`, does the same, but clips the figure to its bounding box.

With the `graphicx` package one may specify a series of options as a key–value list, e.g.:
`\includegraphics[width=15pc]{file}`
`\includegraphics[height=5pc]{file}`
`\includegraphics[scale=0.6]{file}`
`\includegraphics[angle=90,width=20pc]{file}`

See the file `grfguide`, section "Including Graphics Files", of the `graphics` distribution for

all options and a detailed description.

The `epsfig` package mimics the commands familiar from the package with the same name in LaTeX2.09. A PostScript file `file` is included with the command `\psfig{file=file}`.

Grey-scale and colour photographs cannot be included in this way, since reproduction from the printed CRC article would give insufficient typographical quality. See the following subsections.

Figure 1. Good sharp prints should be used and not (distorted) photocopies.

Figure 2. Remember to keep details clear and large enough.

3.5. Black and white photographs

Photographs must always be sharp originals (*not screened versions*) and rich in contrast. They will undergo the same reduction as the text and should be pasted on your page in the same way as line drawings.

3.6. Colour photographs

Sharp originals (*not transparencies or slides*) should be submitted close to the size expected in publication. Charges for the processing and printing of colour will be passed on to the author(s) of the paper. As costs involved are per page, care should be taken in the selection of size and shape so that two or more illustrations may be fitted together on one page. Please contact the Technical Editor in the Camera-Ready Publications Department at Elsevier for a price quotation and layout instructions before producing your paper in its final form.

4. EQUATIONS

Equations should be flush-left with the text margin; LaTeX ensures that the equation is preceded and followed by one line of white space. LaTeX provides the package `fleqn` to get the flush-left effect.

$$H_{\alpha\beta}(\omega) = E_\alpha^{(0)}(\omega)\delta_{\alpha\beta} + \langle\alpha|W_\pi|\beta\rangle \qquad (1)$$

You need not put in equation numbers, since this is taken care of automatically. The equation numbers are always consecutive and are printed in parentheses flush with the right-hand margin of the text and level with the last line of the equation. For multi-line equations, use the `eqnarray` environment. For complex mathematics, use the $\mathcal{AMS}$-LaTeX package.

REFERENCES

1. S. Scholes, Discuss. Faraday Soc. No. 50 (1970) 222.
2. O.V. Mazurin and E.A. Porai-Koshits (eds.), Phase Separation in Glass, North-Holland, Amsterdam, 1984.
3. Y. Dimitriev and E. Kashchieva, J. Mater. Sci. 10 (1975) 1419.

4. D.L. Eaton, Porous Glass Support Material, US Patent No. 3 904 422 (1975).

References should be collected at the end of your paper. Do not begin them on a new page unless this is absolutely necessary. They should be prepared according to the sequential numeric system making sure that all material mentioned is generally available to the reader. Use `\cite` to refer to the entries in the bibliography so that your accumulated list corresponds to the citations made in the text body.

Above we have listed some references according to the sequential numeric system [1–4].